Int J Clin Exp Med 2019;12(7):8149-8160
www.ijcem.com /ISSN:1940-5901/IJCEM0092575

Original Article

Effects of miR-149-3p-mediated PI3K/AKT signaling pathways on proliferation and apoptosis of endothelial cells from hemangioma in children

Xiaoyun Gao[1], Junping Wen[2], Yu Yang[3], Chengyong Huang[4]

Departments of [1]Pediatric Surgery, [2]Endocrinology, [3]Plastic Surgery, [4]Clinical Laboratory, Provincial Clinical College of Fujian Medical University, Fujian Provincial Hospital, Fuzhou 350001, Fujian Province, China

Received February 14, 2019; Accepted March 12, 2019; Epub July 15, 2019; Published July 30, 2019

Abstract: Objective: The aim of the current study was investigate the effects of miR-149-3p-mediated phosphatidylositol-3-kinase/protein kinase B (PI3K/AKT) signaling pathways on proliferation and apoptosis of endothelial cells from hemangiomas in children. Methods: Hemangioma tissues and normal tissues adjacent to cancer from 59 children were collected, detecting expression of protein kinase B (AKT) using immunohistochemistry. Endothelial cells of normal tissues adjacent to cancer (Normal group) and hemangioma tissues were extracted. The latter were divided into the Model group (without any treatment), NC group (transfection of negative plasmid), miR-149-3p mimic group (transfection of miR-149-3p mimic plasmid), miR-149-3p inhibitor group (transfection of miR-149-3p inhibitor plasmid), LY294002 group (inhibitor of PI3K/AKT signaling pathways), and miR-149-3p mimic + LY294002 group. Dual-luciferase report gene assay was used to verify targeted relationships between miR-149-3p and AKT. Quantitative Real-time Polymerase Chain Reaction (qRT-PCR) was used to detect mRNA expression of miR-149-3p, PI3K, AKT, and c-myc. Western blot was used to detect protein expression of PI3K, p-PI3K, AKT, p-AKT, and c-myc. MTT (3-(4,5-dimetyl-2-thiazolyl)-2,5-diphenyl-2-H-tetrazolium bromide, Thiazolyl Blue Tetrazolium Bromide) was used to detect proliferation of cells. Flow cytometry with Annexin V staining was used to detect apoptosis. Results: Positive expression rates of AKT in hemangioma tissues were significantly higher than those in normal tissues ($P<0.05$). According to dual-luciferase report gene assay, AKT was the target gene of miR-149-3p. According to cell experiments, compared with the Normal group, in Model, NC, miR-149-3p mimic, miR-149-3p inhibitor, LY294002, and miR-149-3p mimic + LY294002 groups, mRNA expression of miR-149-3p was decreased. Moreover, mRNA expression of c-myc, PI3K, and AKT, as well as phosphorylation protein expression of PI3K and AKT, was increased. Proliferation was increased but apoptosis was decreased (all $P<0.05$). There were no statistically significant differences in indicators between Model and NC groups (all $P>0.05$). Conclusion: Results suggest that miR-149 inhibits activation of PI3K/AKT signaling pathways in a targeted way, promoting apoptosis and inhibiting proliferation of endothelial cells from hemangiomas in children.

Keywords: miR-149, PI3K/AKT signaling pathway, hemangiomas in children, endothelial cells, proliferation, apoptosis

Introduction

Hemangiomas, a common angiogenic disease in children, are benign tumors of vascular endothelial cells [1]. Some hemangiomas involute by themselves. However, large and fast-growing hemangiomas are prone to ruptures, causing infections, disfigurement, and even coagulation disorders [2]. Currently, pathological mechanisms of proliferation and involution remain unclear in clinical practice. Thus, effective treatments are lacking. Overactivity of blood vessels and excessive proliferation of endothelial cells are the biggest pathological characteristics of hemangiomas in the proliferative phase. Therefore, key points in the treatment of hemangiomas and regression of hemangiomas are the reduction of proliferation and promotion of apoptosis of endothelial cells [3].

PI3K (phosphatidylinositol-3-kinase) is a family containing lipid kinases. After binding to membrane receptors, the ligand of PI3K catalyzes and generates PI3P. It functions as a second

messenger and further activates AKT, a downstream molecule of PI3K [4]. According to a study, PI3K and AKT regulate growth, proliferation, apoptosis, and the glycol-metabolism of cells [5]. According to a study by Pan WK et al., protein expression of PI3K and p-AKT in tissues of children with hemangiomas is significantly higher than that in normal children [6]. According to a study by Zheng N and others, AKT signaling pathways in hemangiomas are overactivated. Inhibiting the activation of this pathway in a targeted way significantly inhibits proliferation of endothelial cells from hemangiomas and growth of hemangiomas [7]. MicroRNAs are endogenous, micromolecular, and non-coding RNAs, which regulate expression of genes and contribute to differentiation, development, and metabolism of cells [8]. In recent years, more and more studies have shown that miR-149-3p is lowly expressed in tumors. For example, Ke Y explored epithelial-mesenchymal transition of non-small cell lung cancer (NSCLC) cells. They found that miR-149-3p targeted to inhibit expression of FOXM1, acting as a tumor suppressor RNA in NSCLC [9]. According to a study by Xue L and others, low expression of miR-149-3p activates AKT signaling pathways to accelerate the progression of gliomas. This is related to poor prognosis of patients [10]. Moreover, miR-149-3p has been confirmed to act together with AKT, regulating cancer progression. However, it remains unclear whether miR-149-3p is associated with hemangiomas in children. Therefore, based on previous studies, miR-149-3p was hypothesized to mediate PI3K/AKT signaling pathways, regulating progression of hemangiomas in children. Therefore, related experiments were carried out.

Materials and methods

Research objects

Hemangioma tissues and normal tissues adjacent to cancer specimens were collected from 59 children pathologically diagnosed and undergoing surgical resections in Fujian Provincial Hospital, Provincial Clinical Medical College of Fujian Medical University, from January 2013 to December 2017. According to Mulliken classification criteria, 21 cases were in the proliferative phase and 38 cases were in the extinction phase [11]. Parts of hemangioma tissue and normal tissue specimens were fixed with 10% neutral formaldehyde solution (Cannice Biomedical Technology Co., Ltd., China) for subsequent experiments. The remaining specimens were washed with PBS solution (Dycent Biotech (Shanghai) Co., Ltd.) at 4°C and stored in liquid nitrogen at -80°C. Inclusion criteria: (1) Children with complete data, diagnosed with hemangiomas by cytology or histology; (2) Children that underwent surgical resections, with biopsy specimens sectioned through clinical evaluation; and (3) Children without other genetic diseases or history of cancer. Exclusion criteria: (1) Children with severe complications; (2) Children with endocrine diseases; (3) Children with incomplete treatment data; and (4) Children with degenerative biopsy specimens during preservation. The use of specimens was agreed upon by the children and their families. This study was approved by the Ethics Committee of Fujian Provincial Hospital, Provincial Clinical Medical College of Fujian Medical University.

Immunohistochemistry

Hemangioma and normal tissue specimens fixed with 10% neutral formaldehyde were embedded in paraffin, with 4 μm serial sections. Tissue sections were baked in an incubator at 60°C for 1 hour, dewaxed with xylene for 1 minute, dehydrated with gradient alcohol for 1 minute, washed with tap water for 1 minute, incubated in 3% H_2O_2 (Jiangmen Hengjian Pharmaceutical Co., Ltd., China) at 37°C for 30 minutes, washed with PBS for 3 minutes, boiled in 0.01 M citric acid buffer (Thermo Fisher Scientific, USA) at 95°C for 20 minutes, cooled to room temperature, washed with PBS, sealed with 100 μL of 5% BSA, and incubated at 37°C for 10 minutes. The sections were then added dropwise with primary antibody rabbit anti-human AKT (1:1,000, Abcam, UK). They stayed at 4°C overnight and were washed with PBS. Afterward, they were added dropwise with horseradish peroxidase-labeled (HRP-labeled) secondary antibody goat anti-rabbit IgG (1:2,000, Shanghai Baiyan Biotechnology Co., Ltd., China), incubated at room temperature for 30 minutes, colored with DAB (Abcam, UK), re-stained with hematoxylin (Beijing Bioss Biotechnology Co., Ltd., China), and sealed. The primary antibody was replaced with PBS as a negative control. A total of 100 cells in five fields (400×) were randomly selected in one section for scoring, according to the percentage of positive

cells: positive cells/all cells * 100% >20% considered as positive (+), and positive cells/all cells * 100% ≤20% as negative (-).

Culturing, morphological observations, and identification of endothelial cells from hemangiomas

Cell culturing: Fresh hemangioma and normal tissues adjacent to cancer tissues were washed with PBS over 5 minutes for a total of 3 times. They were trimmed into tissue masses with 1 mm^3, added with 2 mL of 0.25 trypsin (Procell Life Science & Technology Co., Ltd., Wuhan, China), and digested in a water bath at 37°C for 15 minutes. The trypsin was discarded, adding 4 mL of culture solution containing 10% fetal bovine serum (FBS) (Thermo Fisher Scientific, USA) to terminate digestion. The digested tumor was inoculated in the bottom of the culture flask with 3-5 mm in intervals. It was added with approximately 1 mL of complete endothelial cell culture medium (Sciencell, USA). The flask was inverted into the incubator, incubated at 37°C for 24 hours, and added with 2 mL of complete endothelial cell culture solution. The solution was changed once every two days. The tissue mass was removed one week later. When cell density reached 80%, the cells were passed on. Cultured cells were purified through mechanical curettage, enzyme digestion, and the repeated adherence method.

Morphological observation of endothelial cells from hemangiomas: Morphological changes of the cultured cells were observed under a microscope (Nikon, Japan).

Detection of factor VIII-related antigen by immunohistochemistry (SP method): Endothelial cells were inoculated in a 24-well plate, placed in a round coverslip, cultured for 48 hours, washed with PBS over 5 minutes for a total of 3 times, fixed with 95% ethanol at room temperature for 15 minutes, incubated with 0.3% H_2O_2 at room temperature for 10 minutes, washed with PBS for 3 minutes, and sealed with 100 μL of 5% BSA for 10 minutes. The cells were then added dropwise with rabbit anti-human antibody of factor VIII-related antigen (Shanghai Yuping Biotechnology Co., Ltd., China) at 1:100, stayed at 4°C overnight, and washed with PBS. Afterward, they were added dropwise with HRP-labeled goat anti-rabbit secondary antibody IgG (1:2,000, Shanghai Baiyan Biotechnology Co., Ltd., China), incubated at room temperature for 10 minutes, washed with PBS, added dropwise with streptomycin anti-biotin-peroxidase solution, incubated at room temperature for 10 minutes, washed with PBS, colored with DAB (Abcam, UK), re-stained with hematoxylin, and sealed. Under the microscope, five visual fields (200×) were randomly selected for observation and photographing, calculating the percentage of positive cells: positive cells/all cells * 100%.

Cell transfection and grouping

Endothelial cells in adjacent normal tissues were placed in the Normal group. Endothelial cells from hemangiomas were divided into the Model group (without any treatment), NC group (transfection of negative plasmid), miR-149-3p mimic group (transfection of miR-149-3p mimic plasmid), mir-149-3p inhibitor group (transfection of mir-149-3p inhibitor plasmid), LY294002 group (inhibitor of PI3K/AKT signaling pathways), and miR-149-3p mimic + LY294002 group. Cells were inoculated into a 24-well plate 24 hours before transfection. They were transfected according to the instructions of Lipofectamine 2000 (Shanghai Huiying Biological Technology Co., Ltd., China) when cell density reached 30-50%. Moreover, 100 pmol of negative plasmid, miR-149-3p mimic plasmid, miR-149-3p inhibitor plasmid, and the inhibitor of PI3K/AKT signaling pathways were diluted with 250 μL of serum-free medium Opti-MEM (model: 31985070, Gibco, USA). They were gently mixed and incubated at room temperature for 5 minutes. Next, 5 μL of Lipofectamine 2000 was diluted with 250 μL of serum-free medium Opti-MEM, gently mixed, and incubated at room temperature for 5 minutes. The two materials mentioned above were mixed evenly, incubated at room temperature for 20 minutes, added into wells, and cultured with 5% CO_2 at 37°C. After 6-8 hours, the medium was replaced with a complete medium. After 24-48 hours, subsequent experiments were carried out.

Dual-luciferase report gene assay

The biological prediction website was used to analyze target genes of miR-149-3p, verifying whether AKT was a direct target gene. Luciferase reporter gene assay was used to verify whether AKT was a direct target of miR-149

Table 1. Primer sequences of PCR

Primer	Sequence
Wild type AKT13'-UTR upstream	5'-CTGACTGTCCCACCGGGAGCCTCCCCCTCAGATGATCTCTCCACGGTAGCACTTGACCTTTTCGACC-3'
Wild type AKT13'-UTR downstream	5'-TCGAGGTCGAAAAGGTCAAGTGCTACCGTGGAGAGATCATCTGAGGGGGAGGCTCCCGGTGGGACAGTCAGAGCT-3'
Mutant AKT13'-UTR upstream	5'-CTGACTGTCCCACCGGGAGCCTCCCCCTCAGATGAAGAGAGGTCGGTAGCACTTGACCTTTTCGACC-3'
Mutant AKT13'-UTR downstream	5'-TCGAGGTCGAAAAGGTCAAGTGCTACCGTGGAGAGATCATCTGAGGGGGAGGCTCCCGGTGGGACAGTCAGAGCT-3'

Note: PCR, polymerase chain reaction.

Table 2. Primer sequences of qRT-PCR

Gene	Upstream sequence	Downstream sequence
miR-149-3p	5'-TTTAGGGAGGGACGGGG-3'	5'-GTGCGTGTCGTGGAGTCG-3'
PI3K	5'-CATCACTTCCTCCTGCTCTAT-3'	5'-CAGTTGTTGGCAATCTTCTTC-3'
AKT	5'-GGACAACCGCCATCCAGACT-3'	5'-GCCAGGGACACTCCATCTC-3'
c-myc	5'-TGCTGCATGAAGAGACACCG-3'	5'-TTTCAACTGTTCTCGCCGTT-3'
GAPDH	5'-AGCCACATCGCTCAGACACC-3'	5'-GTACTCAGCGGCCAGCATCG-3'
U6	5'-CTCGGCTTCGGCAGCACA-3'	5'-AACGCTTCACGAATTTGCGT-3'

Note: qRT-PCR, quantitative real-time polymerase chain reaction; PI3K, phosphatidylositol-3-kinase; AKT, protein kinase B.

[12]. Recognition sites of restriction enzymes SpeI and HindIII were introduced into upstream and downstream primers. Te complementary sequence mutation site of the seed sequence was designed on AKT wild type. After restriction enzyme digestion, T4 DNA ligase was used to insert target fragments into the pMIR-reporter. Correctly sequenced luciferase report plasmids WT and MUT were, respectively, co-transfected with miR-149-3p into HEK-293T (Wuhan Yipu Biotechnology Co., Ltd., China). After 48 hours, the cells were collected, lysed, and centrifuged at 2,000 r/min for 5 minutes. The supernatant was taken to detect the fluorescence intensity using a Fluor tester (Promega, USA).

Plasmid construction: The template was the whole blood genome DNA of healthy people, while polymerase chain reaction (PCR) amplification contained AKT1 3'-UTR area of miR-149-3p binding sites. Primers were designed and synthesized according to AKT1 gene 3'UTR sequence and recognition sites of SpeI and HindⅢ were introduced into upstream and downstream primers. PCR primers were synthesized by Shanghai GenePharma Co., Ltd. See **Table 1** for sequences. After enzyme digestion, purification, and recycling, purified and recovered products ligated the inserted fragment at 16°C overnight. These were transformed into DH5α competent cells. After plates were coated, positive mono-clones were selected and cultured in a shake-flask overnight to extract plasmid and conduct PCR. This was identified with enzyme digestion and sent to Invitrogen USA for sequencing. The plasmid containing the correct target sequence was named as a wild type. With the wild type as a template, miR-149-3p and AKT1 3'-UTR area were bound to the base and mutated into a meaningless sequence. Site-directed mutant primers were designed (See **Table 1**), with specific operations in accord with instructions. The successful mutant plasmid was named as a mutant. It was sequenced after PCR, identifying with enzyme digestion. The above plasmids were purchased from Promega, USA [13].

qRT-PCR

After 48 hours, total RNA and tissues were extracted, according to manufacturer instructions of TRIzol (Thermo Fisher Scientific, USA). Concentrations and purities of RNA were detected using an ultraviolet spectrophotometer (Beijing Mairuibo Biotechnology Co., Ltd., China). Samples with a purity of A260/A280 = 1.8-2.0 were adjusted to 50 ng/μL. PrimeScriptTM RT reagent Kit (Takara, Japan) was used to reversely transcribe RNA into cDNA (50 ng/μL), which was frozen at -80°C for use. With reference to GenBank database, primers were designed using the Primer 5.0 computer software and synthesized by Annoron Biotechnology Co., Ltd. (See **Table 2**). According to ABI 7900HT Quantitative Real-time Polymerase Chain Reaction (qRT-PCR), GAPDH and U6 served as internal references. Reaction conditions were pre-denaturation at 95°C for 30 seconds, degeneration at 95°C for 5 seconds, annealing at 58°C for 30 seconds, and extension at 72°C for 15 seconds, for 40 cycles. Relative expres-

sion of miR-149, PI3K, AKT, and c-myc mRNA was calculated using $2^{-\Delta\Delta Ct}$ and the formulas were: $\Delta Ct = Ct_{target\ gene} - Ct_{internal\ reference\ gene}$, $\Delta\Delta Ct = \Delta Ct_{treatment\ group} - \Delta Ct_{control\ group}$. Three same wells were set for each gene in the samples.

Western blotting

After 48 hours, total proteins were extracted using the protein extraction kit (Bestbio, Shanghai). Phosphorylated proteins were extraced using phosphorylated protein extraction kit (Beijing Biolab Technology Co., Ltd., China). Concentrations of protein samples were determined using the BCA kit (Pierce, USA), with 10% SDS-PAGE gel (Beyotime Institute of Biotechnology, China) prepared. A total of 50 μg of protein samples was added to each well, separated by electrophoresis, transferred to PVDF membranes, and sealed with TBST buffer containing 5% skim milk powder for 2 hours. After washing with TBST, the membrane was added dropwise with primary antibodies rabbit anti-human PI3K (1:1,000, abcam, UK), p-PI3K (1:1,000, abcam, UK), AKT (1:500, abcam, UK), p-AKT (1:500), c-myc (1:1,000 abcam, UK), and GAPDH (1:10,000, abcam, UK), all of which were purchased from Abcam, UK. The membrane was incubated at 4°C overnight, rinsed with PBST over 10 minutes for 3 times, added with peroxidase-labeled goat anti-rabbit IgG (1:2,000, Shanghai Baiyan Biotechnology Co., Ltd., China) as a secondary antibody, incubated at room temperature for 1 hour, washed with TBST over 10 minutes for 3 times, colored in ECL reaction solution (Millipore, USA), exposed in a cassette, and developed. With GAPDH as an internal reference, relative expression of proteins = the gray value of the target protein/the gray value of GAPDH. The gray value of the target band was analyzed using Western blot analysis software Image J (National Institutes of Health, USA).

MTT

After 48 hours, cells were inoculated in a 96-well plate with $3*10^3$ - $6*10^3$ cells and 0.1 mL per well for 6 wells. They were incubated in an incubator for 24, 48, and 72 hours, with the following experiments carried out. A total of 20 μL of prepared MTT solution (Beijing Solarbio Science & Technology Co., Ltd., China) at 5 mg/mL was added to each well and incubated at 37°C for 2 hours. Afterward, the supernatant was aspirated and discarded and 150 μL of DMSO was added to each well to measure the OD value at 490 nm using an ELISA detector (Beijing Nuoyawei Instruments Co., Ltd., China).

Flow cytometry

After 48 hours, the cells were digested with trypsin without EDTA, collected in a flow tube, and centrifuged. The supernatant was discarded. They were washed with cold PBS over 5 minutes for 3 times and centrifuged at 2,000 r/min, with the supernatant discarded. According to instructions for the Annexin-V-FITC cell apoptosis detection kit (Dalian Melonepharma Technology Co., Ltd., China), Annexin-V-FITC, PI and HEPES buffer were prepared into Annexin-V-FITC/PI dye liquor at 1:2:50. A total of $1*10^6$ cells were resuspended with 100 μL of dye liquor, mixed evenly by shaking, incubated at room temperature for 15 minutes, added with 1 mL of HEPES buffer, and mixed evenly by shaking. Flow cytometer (BD, USA) excited band-pass filters with 525 nm and 620 nm at 488 nm were used to detect FITC and PI fluorescence, respectively, as well as apoptosis.

Statistical analysis

Statistical data were processed and analyzed using SPSS statistical software, version 21.0. Measurement data are expressed by mean ± standard deviation ($\bar{x} \pm sd$). Multiple groups of data were compared by analysis of variance (ANOVA) and tested by homogeneity of variance. When ANOVA was significantly different, q-test was used for pairwise comparisons. When the variance was unequal, a nonparametric rank test was used. $P<0.05$ indicates statistically significant differences.

Results

General information

Based on general information, the 59 children with hemangiomas in this study consisted of 32 males and 27 females, aged from 3 months to 4 years. Based on hemangioma sites, 24 cases had hemangiomas in the lips and cheeks, 6 cases were in the nose, 12 cases were in the limbs, 8 cases were in the back, 4 cases were in the chest, and 5 cases were in the abdomen. Based on hemangioma area, the smallest hemangioma was 1.5 cm*2 cm and the largest was

Table 3. General information

Item	Case (n)
Gender	
Male	32
Female	27
Age	3 months - 4 years old
Hemangioma sites	
Lip and cheek	24
Nose	6
Limbs	12
Back	8
Chest	4
Abdomen	5
Hemangioma area	
Smallest	1.5 cm*2 cm
Largest	2.5 cm*4 cm
Mulliken classification	
Proliferative phase	21
Involuting phase	38

2.5 cm*4 cm. Based on Mulliken classification, 21 cases were in the proliferative phase and 38 cases in the involuting phase. See **Table 3** for more details.

Immunohistochemical detection of positive expression of AKT protein in hemangiomas and normal tissues

According to immunohistochemistry (**Figure 1**), AKT was positively expressed in the cytoplasm and the positive particles were brownish yellow. The positive expression rate of AKT protein was (14.11±2.32)% in normal tissues adjacent to cancer tissues, significantly lower than the (53.16±6.13)% found in hemangioma tissues, with statistically significant differences ($P< 0.05$).

Morphological observation and identification of endothelial cells from hemangiomas

After inoculation for 3 to 5 days, endothelial cells from hemangiomas crawled out of the tissue mass and swam out from the edge of it. They were round, oval, or polygonal, with intact cytomembranes. There was a round or oval nucleus under the microscope. After culturing for 2-3 weeks, endothelial cells spread all over the bottom of the culture flask and grew in a vortex way, arranging in a "pebble shape". Factor VIII-related antigen was mainly expressed in the cytoplasm and cytomembranes of endothelial cells from hemangiomas, with obvious brownish yellow particles and a positive expression rate of more than 95%. According to the morphological characteristics of cells under the microscope and results of immunohistochemical staining, the cultured cells had endothelial cell specificity. They were endothelial cells from hemangiomas. See **Figure 2**.

Dual luciferase reporter gene assay

According to online analysis software, there was a specific binding domain between AKT and miR-149-3p sequences. AKT was identified as the target gene of miR-149-3p (**Figure 3A**). According to luciferase reporter gene assay, the luciferase signal of the Wt-miR-149-3p/AKT co-transfection group in the miR-149-3p mimic group was lower than that in the NC group ($P<0.05$), without significant differences in the luciferase activity of Mut-3'UTR between the two groups ($P>0.05$). Results indicate that miR-149-3p can specifically bind to AKT, the target gene of miR-149-3p.

Detection of mRNA expression of miR-149-3p, PI3K, AKT, and c-myc by qRT-PCR

According to qRT-PCR (**Figure 4**), compared with the Normal group, mRNA expression of miR-149-3p was decreased. However, that of c-myc, PI3K, and AKT was increased in Model, NC, miR-149-3p mimic, miR-149-3p inhibitor, LY294002, and miR-149-3p mimic + LY294002 groups (all $P<0.05$). Compared with the Model group, mRNA expression of miR-149-3p was increased. However, that of c-myc, PI3K, and AKT was decreased in the miR-149-3p mimic and miR-149-3p mimic + LY294002 groups (all $P<0.05$). Moreover, mRNA expression of c-myc, PI3K, and AKT in the LY294002 group was decreased (all $P<0.05$), without statistically significant differences, compared to that of miR-149-3p ($P>0.05$). Also, mRNA expression of miR-149-3p in the miR-149-3p inhibitor group was decreased. However, that of c-myc, PI3K, and AKT was increased in the miR-149-3p inhibitor group (all $P<0.05$). There were no significant differences in expression of genes between the Model and NC groups (all $P>0.05$). Compared with the miR-149-3p mimic group, mRNA expression of miR-149-3p was decreased in the LY294002 group ($P<0.05$), without significant differences compared to that of

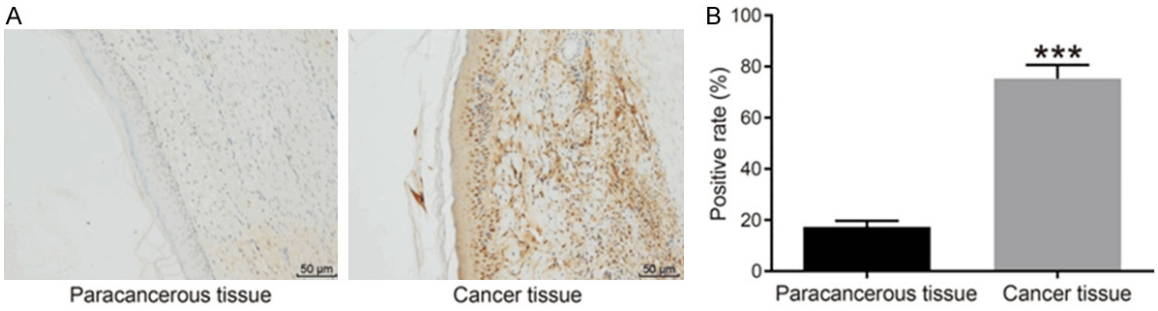

Figure 1. Immunohistochemical staining. Para-cancerous tissue was the normal tissue adjacent to cancer tissue and cancer tissue was hemangioma tissue. A: Immunohistochemical staining (200×). B: Histogram of the positive expression rate of AKT protein. Compared with the normal tissue adjacent to cancer, ***P<0.001.

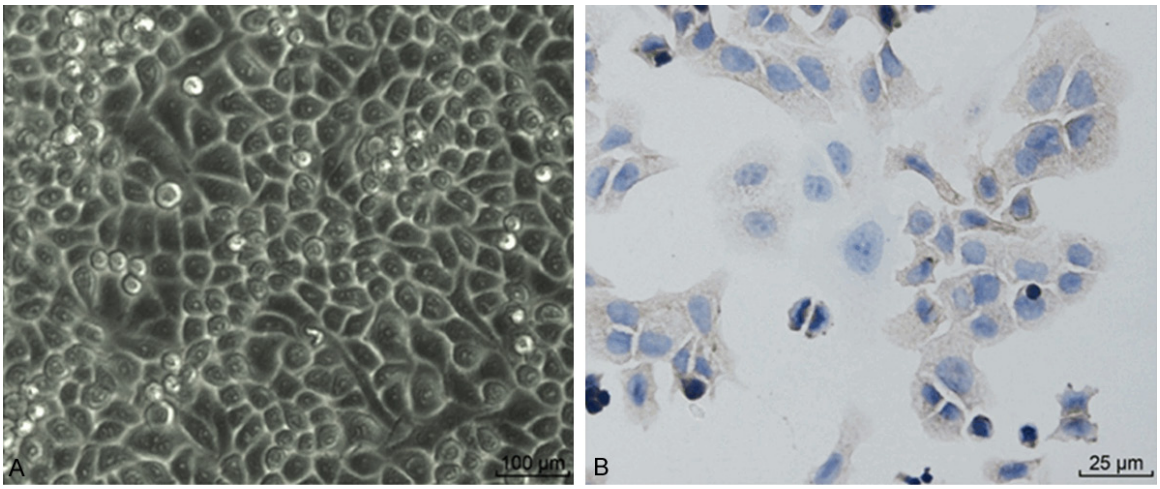

Figure 2. Morphological observation and immunohistochemistry of endothelial cells from hemangioma. A: Cells covered with the culture flask after culture for 3 weeks (100×). B: The staining of factor VIII-related antigen of hemangioma cells (immunohistochemistry, 400×).

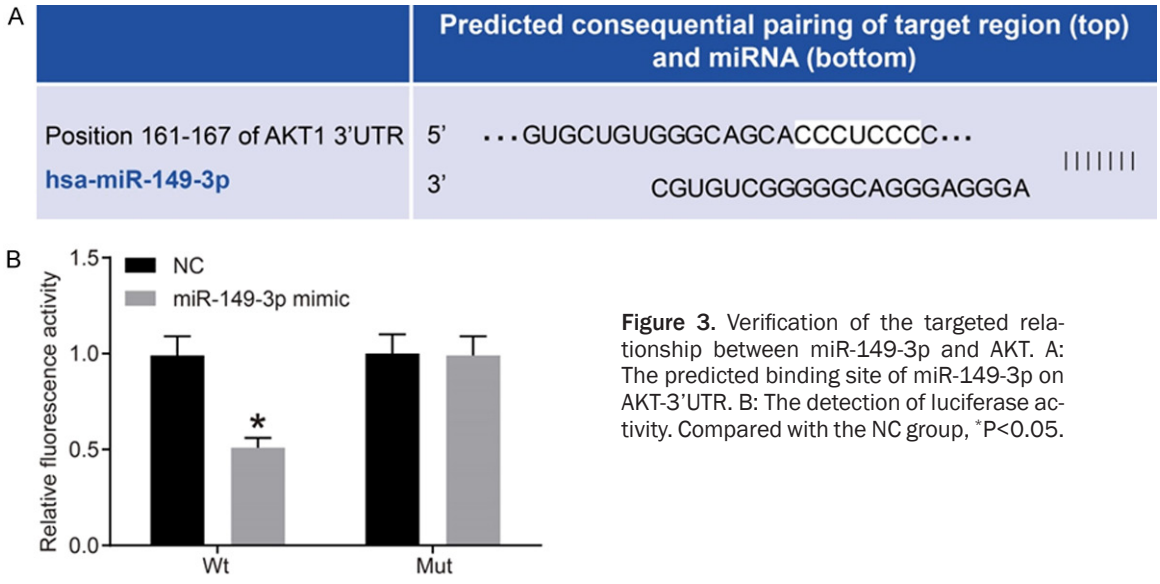

Figure 3. Verification of the targeted relationship between miR-149-3p and AKT. A: The predicted binding site of miR-149-3p on AKT-3'UTR. B: The detection of luciferase activity. Compared with the NC group, *P<0.05.

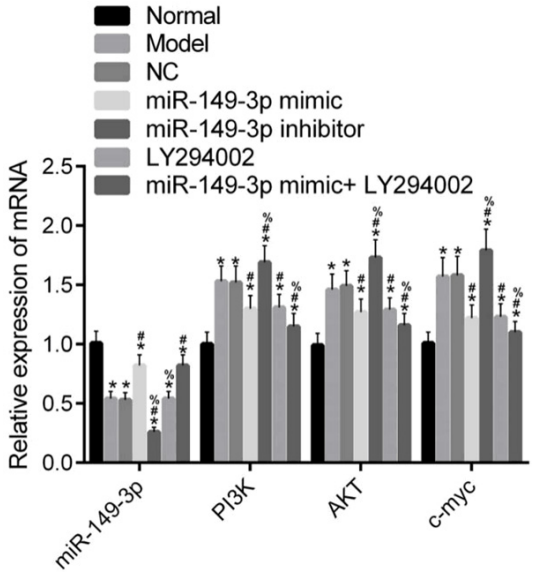

Figure 4. Comparison of mRNA expression of miR-149-3p, PI3K, AKT, and c-myc. Compared with the Normal group, *P<0.05; compared with the Model group, #P<0.05; compared with the miR-149-3p mimic group, %P<0.05. PI3K, phosphatidylositol-3-kinase; AKT, protein kinase B.

other genes (all P>0.05). Furthermore, mRNA expression of c-myc, PI3K, and AKT in the miR-149-3p mimic + LY294002 group was decreased (all P<0.05), without significant differences compared to that of miR-149-3p (P> 0.05). Finally, mRNA expression of miR-149-3p in the miR-149-3p inhibitor group was decreased. However, that of c-myc, PI3K, and AKT was increased (all P<0.05).

Detection of protein expression of PI3K, p-PI3K, AKT, p-AKT, and c-myc by Western blotting

According to Western blotting (**Figure 5**), compared with the Normal group, protein expression of c-myc, PI3K, p-PI3K, AKT, and p-AKT was increased in Model, NC, miR-149-3p mimic, miR-149-3p inhibitor, LY294002, and miR-149-3p mimic + LY294002 groups (all P<0.05). Compared with the Model group, protein expression in miR-149-3p mimic and miR-149-3p mimic + LY294002 groups was decreased (all P<0.05). Protein expression in the LY294002 group was decreased (all P<0.05). Protein expression in the miR-149-3p inhibitor group was increased (all P<0.05). There were no significant differences in protein expression between Model and NC groups (all P>0.05). Compared with the miR-149-3p mimic group, protein expression in the LY294002 group was not significantly different (all P>0.05). Protein expression in the miR-149-3p mimic + LY294002 group was decreased (all P<0.05). Protein expression in the miR-149-3p inhibitor group was increased (all P<0.05).

Detection of proliferation of cells by MTT

According to MTT (**Figure 6**), there were no significant differences in OD values between the groups at 24 hours (all P>0.05). At 48 and 72 hours, compared with the Normal group, OD values in the Model, NC, miR-149-3p mimic, miR-149-3p inhibitor, LY294002, and miR-149-3p mimic + LY294002 groups were increased (all P<0.05). At 48 and 72 hours, compared with the Model group, OD values in the miR-149-3p inhibitor group were increased (both P<0.05). Levels were decreased in the miR-149-3p mimic, LY294002, and miR-149-3p mimic + LY294002 groups (all P<0.05). There were no significant differences between Model and NC groups at each time point (both P>0.05). At 48 and 72 hours, compared with the miR-149-3p mimic group, OD values in the LY294002 group were not significantly different (all P>0.05), but were decreased in the miR-149-3p mimic + LY294002 group (all P<0.05).

Detection of apoptosis by flow cytometry

According to flow cytometry (**Figure 7**), compared with the Normal group, apoptosis rates in Model, NC, miR-149-3p mimic, miR-149-3p inhibitor, LY294002, and miR-149-3p mimic + LY294002 groups were decreased significantly (all P<0.05). Compared with the Model group, apoptosis rates in the miR-149-3p inhibitor group were decreased significantly (P<0.05), but were increased significantly in the miR-149-3p mimic, LY294002, and miR-149-3p mimic + LY294002 groups (all P<0.05). There were no statistically significant differences between Model and NC groups (P>0.05). Compared with the miR-149-3p mimic group, apoptosis rates in the miR-149-3p inhibitor group were decreased significantly (P<0.05), but were increased significantly in the miR-149-3p mimic + LY294002 group (P<0.05). There were no significant differences between miR-149-3p mimic and LY294002 groups (P>0.05).

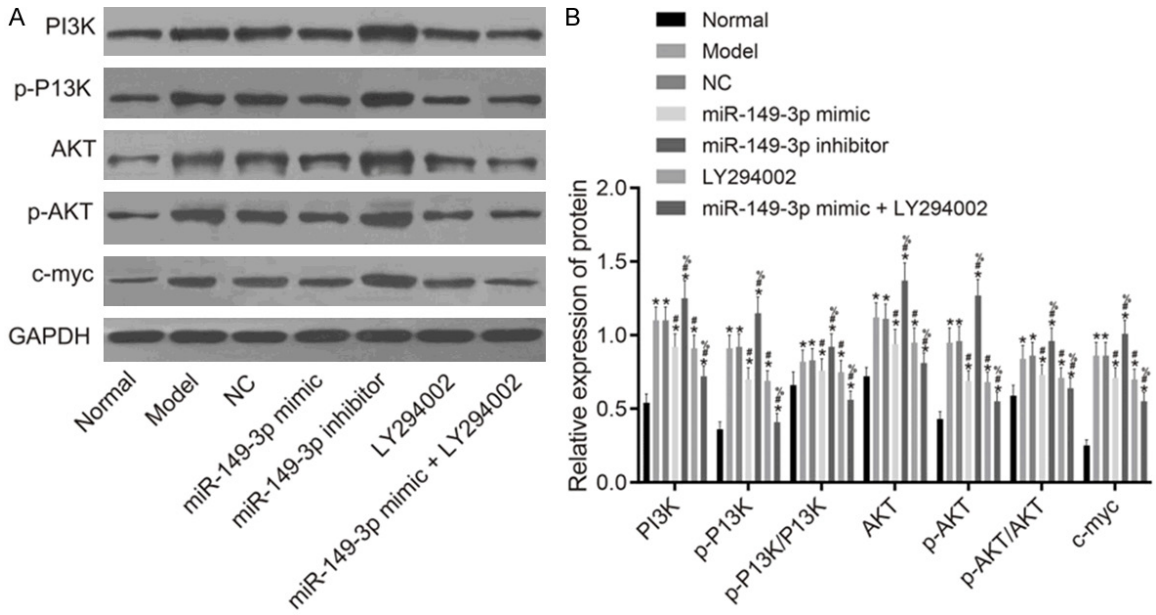

Figure 5. Comparison of protein expression of PI3K, p-PI3K, AKT, p-AKT, and c-myc. A: Protein band; B: Protein expression histogram. Compared with the Normal group, *P<0.05; compared with the Model group, #P<0.05; compared with the miR-149-3p mimic group, %P<0.05. PI3K, phosphatidylositol-3-kinase; AKT, protein kinase B.

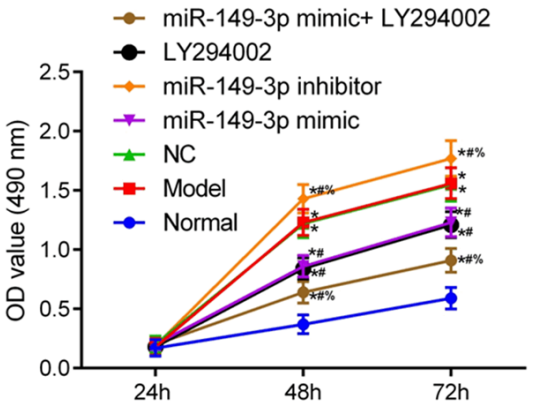

Figure 6. Comparison of cell proliferation ability. Compared with the Normal group, *P<0.05; compared with the Model group, #P<0.05; compared with the miR-149-3p mimic group, %P<0.05. OD, optical density.

Discussion

Recent studies have confirmed that PI3K/AKT signaling pathways play an important role in cell metabolism, cell cycle control, angiogenesis, and chemotherapy resistance [14-16]. AKT, a downstream molecule of PI3K, is an important check point of PI3K/AKT signaling pathways. Its phosphorylation is an important marker for activation of this pathway [17, 18]. Li and others have explored the relationship between hemangiomas in children and PI3K/AKT signaling pathways, finding that phosphorylation of AKT can activate its downstream mTOR protein, accelerate cell progression from G1 to S phases, and promote proliferation of hemangioma cells [19]. Immunohistochemistry was used in this study to observe positive expression of AKT in hemangioma and normal tissues. Positive expression of AKT found in hemangioma tissues was significantly increased, confirming that AKT might be related to the pathogenesis of hemangiomas.

Moreover, miR-149-3p has been proven to play a protective role in cancers. For example, Cao found that glycyrrhetinic acid inhibits the progression of gastric cancer through activating miR-149-3p-Wnt signaling pathways [20]. Studying the biological characteristics of bladder cancer cells, Yang confirmed that miR-149-3p inhibits S100A4 in a targeted way, thereby inhibiting proliferation, migration, and invasion of bladder cancer cells [21]. Additionally, there is a study confirming that miR-149 inhibits the growth and metastasis of NSCLC by inhibiting the FOXM1/cyclin D1/MMP2 axis [22]. These studies have confirmed the protective role of miR-149 in cancer progression. The current study verified the targeted relationship between miR-149 and AKT through dual luciferase report

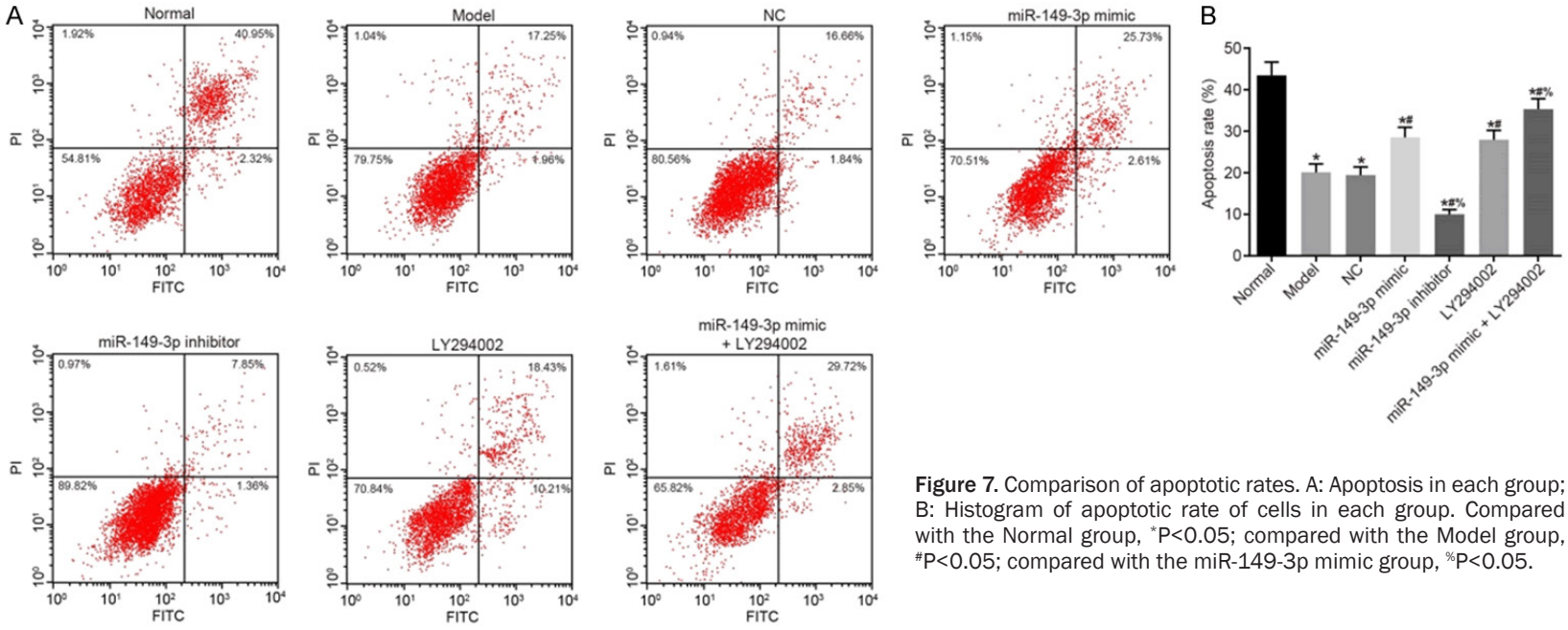

Figure 7. Comparison of apoptotic rates. A: Apoptosis in each group; B: Histogram of apoptotic rate of cells in each group. Compared with the Normal group, *P<0.05; compared with the Model group, #P<0.05; compared with the miR-149-3p mimic group, %P<0.05.

gene assay. Additionally, qRT-PCR was used to observe expression of miR-149. Compared with the Normal group, expression of miR-149-3p was significantly decreased. However, mRNA and protein expression of PI3K, p-PI3K, AKT, and p-AKT was significantly increased in other groups, proving that PI3K/AKT signaling pathways are significantly activated in hemangioma cells of children. Compared with the Model group, expression of PI3K, p-PI3K, AKT, and p-AKT in the miR-149-3p inhibitor group was increased, indicating that miR-149-3p knockout can promote activation of PI3K/AKT signaling pathways.

As a proto-oncogene, c-myc has been proven to be involved in the gene control of cells, accelerating the transformation of cells into malignant phenotypes [23, 24]. Studies have found that expression of c-myc is abnormally increased in lung cancer, liver cancer, breast cancer, and thyroid cancer [25-28]. Expression of c-myc in other groups was significantly higher than that in the Normal group. Overexpression of miR-149-3p or inhibiting activation of PI3K/AKT signaling pathways reduced its expression, further confirming the protective roles of miR-149 overexpression and inhibiting activation of PI3K/AKT signaling pathways in hemangiomas in children. MTT and flow cytometry were used to detect proliferation and apoptosis of cells. Compared with the normal group, proliferation was significantly enhanced but apoptosis was weakened in other groups. Overexpression of miR-149-3p or inhibiting activation of PI3K/AKT signaling pathways can inhibit proliferation and promote apoptosis of endothelial cells from hemangiomas. The combination of the two is more effective. This study explored the relationship between miR-149-3p, PI3K/AKT signaling pathways, and the biological characteristics of endothelial cells from hemangiomas in children. However, it needs to be further verified whether miR-149-3p and this pathway are affected by related target genes. In addition, experimental conditions may have affected the results of this study.

In summary, miR-149-3p can inhibit expression of AKT in a targeted way and mediate PI3K/AKT signaling pathways, thus promoting apoptosis and inhibiting proliferation of endothelial cells from hemangiomas. This plays a protective role in children with hemangiomas. Moreover, miR-149-3p is expected to become a potential target for treatment of hemangiomas in children.

Acknowledgements

This work was supported by Fujian Provincial Medical Innovation Course for *the influence of PI3K/AKT/mTOR/4EBP1 signaling pathway on occurrence and development of pediatric hemangioma* (2016-CX-6).

Disclosure of conflict of interest

None.

Address correspondence to: Junping Wen, Department of Endocrinology, Provincial Clinical College of Fujian Medical University, Fujian Provincial Hospital, No.134 East Street, Fuzhou 350001, Fujian Province, China. Tel: +86-13559925729; E-mail: wenjunping52@163.com

References

[1] Prey S, Voisard JJ, Delarue A, Lebbe G, Taieb A, Leaute-Labreze C and Ezzedine K. Safety of propranolol therapy for severe infantile hemangioma. JAMA 2016; 315: 413-415.

[2] Munabi NC, England RW, Edwards AK, Kitajewski AA, Tan QK, Weinstein A, Kung JE, Wilcox M, Kitajewski JK, Shawber CJ and Wu JK. Propranolol targets hemangioma stem cells via cAMP and mitogen-activated protein kinase regulation. Stem Cells Transl Med 2016; 5: 45-55.

[3] Zuccolo E, Bottino C, Diofano F, Poletto V, Codazzi AC, Mannarino S, Campanelli R, Fois G, Marseglia GL, Guerra G, Montagna D, Laforenza U, Rosti V, Massa M and Moccia F. Constitutive store-operated Ca(2+) entry leads to enhanced nitric oxide production and proliferation in infantile hemangioma-derived endothelial colony-forming cells. Stem Cells Dev 2016; 25: 301-319.

[4] Dolly SO, Wagner AJ, Bendell JC, Kindler HL, Krug LM, Seiwert TY, Zauderer MG, Lolkema MP, Apt D, Yeh RF, Fredrickson JO, Spoerke JM, Koeppen H, Ware JA, Lauchle JO, Burris HA 3rd and de Bono JS. Phase I study of apitolisib (GDC-0980), dual phosphatidylinositol-3-kinase and mammalian target of rapamycin kinase inhibitor, in patients with advanced solid tumors. Clin Cancer Res 2016; 22: 2874-2884.

[5] Yang W, Hosford SR, Dillon LM, Shee K, Liu SC, Bean JR, Salphati L, Pang J, Zhang X, Nannini MA, Demidenko E, Bates D, Lewis LD, Marotti JD, Eastman AR, Miller TW. Strategically timing inhibition of phosphatidylinositol 3-kinase to maximize therapeutic index in estrogen receptor alpha-positive, PIK3CA-mutant breast cancer. Clin Cancer Res 2016; 83: 1999.

[6] Pan WK, Li P, Guo ZT, Huang Q and Gao Y. Propranolol induces regression of hemangioma cells via the down-regulation of the PI3K/Akt/eNOS/VEGF pathway. Pediatr Blood Cancer 2015; 62: 1414-1420.
[7] Zheng N, Ding X, Sun A and Jahan R. PDK1 activity regulates proliferation, invasion and growth of hemangiomas. Cell Physiol Biochem 2015; 36: 1903-1910.
[8] Huang C, Huang J, Ma P and Yu G. microRNA-143 acts as a suppressor of hemangioma growth by targeting Bcl-2. Gene 2017; 628: 211-217.
[9] Ke Y, Zhao W, Xiong J and Cao R. miR-149 Inhibits Non-Small-Cell Lung Cancer Cells EMT by Targeting FOXM1. Biochem Res Int 2013; 2013: 506731.
[10] Xue L, Wang Y, Yue S and Zhang J. Low MiR-149 expression is associated with unfavorable prognosis and enhanced Akt/mTOR signaling in glioma. Int J Clin Exp Pathol 2015; 8: 11178-11184.
[11] Mulliken JB and Glowacki J. Hemangiomas and vascular malformations in infants and children: a classification based on endothelial characteristics. Plast Reconstr Surg 1982; 69: 412-422.
[12] Li XY, Luo QF, Wei CK, Li DF, Li J and Fang L. MiRNA-107 inhibits proliferation and migration by targeting CDK8 in breast cancer. Int J Clin Exp Med 2014; 7: 32-40.
[13] Collin SP. Topographic organization of the ganglion cell layer and intraocular vascularization in the retinae of two reef teleosts. Vision Res 1989; 29: 765-775.
[14] Yang SX, Polley E and Lipkowitz S. New insights on PI3K/AKT pathway alterations and clinical outcomes in breast cancer. Cancer Treat Rev 2016; 45: 87-96.
[15] Zhang D, Sun G, Zhang H, Tian J and Li Y. Long non-coding RNA ANRIL indicates a poor prognosis of cervical cancer and promotes carcinogenesis via PI3K/Akt pathways. Biomed Pharmacother 2017; 85: 511-516.
[16] Erdogan S, Doganlar O, Doganlar ZB, Serttas R, Turkekul K, Dibirdik I and Bilir A. The flavonoid apigenin reduces prostate cancer CD44(+) stem cell survival and migration through PI3K/Akt/NF-kappaB signaling. Life Sci 2016; 162: 77-86.
[17] Dey N, De P and Leyland-Jones B. PI3K-AKT-mTOR inhibitors in breast cancers: from tumor cell signaling to clinical trials. Pharmacol Ther 2017; 175: 91-106.
[18] Baek SH, Ko JH, Lee JH, Kim C, Lee H, Nam D, Lee J, Lee SG, Yang WM, Um JY, Sethi G and Ahn KS. Ginkgolic acid inhibits invasion and migration and TGF-beta-induced EMT of lung cancer cells through PI3K/Akt/mTOR inactivation. J Cell Physiol 2017; 232: 346-354.
[19] Li D, Li P, Guo Z, Wang H and Pan W. Downregulation of miR-382 by propranolol inhibits the progression of infantile hemangioma via the PTEN-mediated AKT/mTOR pathway. Int J Mol Med 2017; 39: 757-763.
[20] Cao D, Jia Z, You L, Wu Y, Hou Z, Suo Y, Zhang H, Wen S, Tsukamoto T, Oshima M, Jiang J and Cao X. 18beta-glycyrrhetinic acid suppresses gastric cancer by activation of miR-149-3p-Wnt-1 signaling. Oncotarget 2016; 7: 71960-71973.
[21] Yang D, Du G, Xu A, Xi X and Li D. Expression of miR-149-3p inhibits proliferation, migration, and invasion of bladder cancer by targeting S100A4. Am J Cancer Res 2017; 7: 2209-2219.
[22] Zhao L, Liu L, Dong Z and Xiong J. miR-149 suppresses human non-small cell lung cancer growth and metastasis by inhibiting the FOXM1/cyclin D1/MMP2 axis. Oncol Rep 2017; 38: 3522-3530.
[23] Qiu MK,Wang SQ, Pan C. ROCK inhibition as a potential therapeutic target involved in apoptosis in hemangioma. Oncol Rep 2017; 37: 2987-2993.
[24] Zhang HF, Wu C, Alshareef A, Gupta N, Zhao Q, Xu XE, Jiao JW, Li EM, Xu LY and Lai R. The PI3K/AKT/c-MYC axis promotes the acquisition of cancer stem-like features in esophageal squamous cell carcinoma. Stem Cells 2016; 34: 2040-2051.
[25] Ritorto MS, Rhode H, Vogel A, Borlak J. Regulation of glycosylphosphatidylinositol-anchored proteins and GPI-phospholipase D in a c-Myc transgenic mouse model of hepatocellular carcinoma and human HCC. Biol Chem 2016; 397: 1147-1162.
[26] Fan W, Yang H, Liu T, Wang J, Li TW, Mavila N, Tang Y, Yang J, Peng H, Tu J, Annamalai A, Noureddin M, Krishnan A, Gores GJ, Martinez-Chantar ML, Mato JM and Lu SC. Prohibitin 1 suppresses liver cancer tumorigenesis in mice and human hepatocellular and cholangiocarcinoma cells. Hepatology 2017; 65: 1249-1266.
[27] Pourteimoor V, Paryan M and Mohammadi-Yeganeh S. microRNA as a systemic intervention in the specific breast cancer subtypes with C-MYC impacts; introducing subtype-based appraisal tool. J Cell Physiol 2018; 233: 5655-5669.
[28] Cabibi D, Pipitone G, Porcasi R, Ingrao S, Benza I, Porrello C, Cajozzo M and Giannone AG. Pleural epithelioid angiosarcoma with lymphatic differentiation arisen after radiometabolic therapy for thyroid carcinoma: immunohistochemical findings and review of the literature. Diagn Pathol 2017; 12: 60.